P11R.1

FREEZING DRIZZLE DETECTION WITH WSR-88D RADARS

Kyoko Ikeda, Roy M. Rasmussen, and Edward A. Brandes
National Center for Atmospheric Research, Boulder, Colorado

1. Introduction

Freezing drizzle represents a significant in-flight icing hazard and can even cause extensive engine damage to aircraft on the ground. In this paper, we establish a few criteria for detecting freezing drizzle based on WSR-88D radar data. Data analyzed were obtained from a number of freezing drizzle events that occurred at six selected operational radar sites. Radar returns are characterized by the areal-average and standard deviation of radar reflectivity factor as well as the texture of the reflectivity field computed from a Radar Echo Classifier algorithm.

Freezing drizzle typically forms via the collision-coalescence process rather than the classical melting process. Consequently, a reflectivity bright band is generally absent making detection difficult. The similarity of echo structures in freezing drizzle and light snow is also a problem for detection techniques based solely on radar reflectivity. In this study, we compare characteristic radar echo patterns in freezing drizzle and light snow using additional insights gained from cloud top temperatures. The ensemble dataset showed that freezing drizzle may be detected from criteria based on cloud top temperatures and radar echo patterns for single-layered clouds. In other conditions, e.g., in the presence of multiple cloud layers and mixed-phase precipitation, polarimetric-based discrimination of hydrometeors may be more useful because snow particles and drizzle drops have characteristic polarimetric radar returns (Reinking et al. 1997; Ryzhkov and Zrnic1998). Example data obtained with NCAR's dual-polarimetric radar is presented here.

Section 2 gives a description of the dataset. The evolutions of radar echo signatures in freezing drizzle and light snow are discussed in section 3 from example cases and examines these precipitation signatures from an ensemble dataset. Prospects of enhanced freezing-drizzle detection with a polarimetric WSR-88D is discussed in section 4 followed by summary and concluding remarks (Section 5).

2. Data

Radar data were collected in clear-air mode with seven operational WSR-88D radar systems [Denver, CO (KFTG); Pueblo, CO (KPUX); Goodland, KS (KGLD); Minneapolis, MN (KMPX); Duluth, MN (KDLH); Cleveland, OH (KCLE); and Detroit, MI (KDTX)]. These locations were selected because they are climatologically favorable for freezing precipitation (Bernstein 2000). Datasets are in the Level II-format obtained with the 1.5^o antenna elevation. The equivalent radar reflectivity (reflectivity or Z, hereafter) is averaged over a 15-km radius circular area centered at each site. The 1.5^o elevation radar beams are approximately 550 m above the ground at a range of 15 km assuming a standard atmosphere. The average reflectivity ($\overline{Z}$) and associated standard deviations (σ_Z) are assumed to represent precipitation at the surface. Data from the 1.5^o elevation scans were chosen because they were less influenced by ground targets. Reflectivity bright bands can potentially skew the statistical values. Generally, the data did not contain a bright band due to the formation of drizzle from the collision-coalescence process. All statistical values were computed in linear space.

In addition to the spatial average and standard deviation of Z, the texture of the Z field were examined. The reflectivity texture is computed from a Radar Echo Classifier algorithm (Kessinger et al. 2003), and it is the mean squared difference of the Z at each range gate over a small area. The small areas consist 5 beams and the number of gate equivalent to 4-km along-radial distances centered at each range gate. The texture field represents spatial distribution of uniformity/non-uniformity in Z. Although it is a measure of smoothness, the definition is slightly different from the reflectivity texture parameter used in the hydrometeor classification scheme described in Ryzhkov et al. (2005).

Cloud top temperature from infrared satellite and surface conditions from METAR and 1-minute Automated Surface Observation Systems (ASOS) supplement the data.

3. Freezing drizzle detections with WSR-88D radars

a. Examples of freezing drizzle detections at KFTG

Radar signatures of freezing drizzle evolve uniquely under various weather conditions. In the following, data from precipitation events over the Front Range regions of Colorado on 4 March 2003, 30-31 October 2003, 4 January 2005, and 16 February 2005 are described. The precipitation events included a transition from freezing drizzle to light snow and/or light snow to freezing drizzle. Thus, the data are also used to contrast radar echo characteristics in freezing drizzle

* *Corresponding author address:* Kyoko Ikeda, National Center for Atmospheric Research, P.O. Box 3000, Boulder, CO 80307
E-mail: kyoko@ncar.ucar.edu

and light snow—two precipitation types that are often difficult to distinguish.

Precipitation on 4 March 2003 started as freezing drizzle and later changed to light snow from a shallow orographic cloud. Fig. 1 shows a storm vertical structure at KFTG as inferred from Z and the texture of Z. Freezing drizzle was reported at the surface between 1100 and 1430 UTC when reflectivity was typically less than 0 dBZ. The texture field and σ_Z were small indicating a small spatial variation in the reflectivity field (6.31 dBZ^2 and 3-5 dBZ, respectively). A transition from freezing drizzle to light snow was associated with an increase in $\overline{Z}$ to >10dBZ and an increase in σ_Z by 2 dBZ (Fig. 1; after 1430 UTC). The surface precipitation reports given during this time were –fzdzsn (freezing drizzle with light snow). This coincided with an increasing frequency of ice/snow generating cell-like structures aloft and advecting snow bands over the circular domain. Higher texture values below 2 km MSL after 1430 UTC infer that the horizontal Z structure became less uniform (Fig. 1). The CTT cooled from –5^{o}C at 1200 UTC to –15^{o}C by 1500 UTC as the cloud layer slowly deepened; thus the nucleation of ice likely became more active (Geresdi et al. 2005) leading to a loss of the echo uniformity. Later, a decrease in σ_Z to 2-3 dBZ occurred as the low-level cloud became much more stratiform (Fig. 1; after 1700 UTC).

Much stronger reflectivity (i.e., higher snowfall rate) after 1800 UTC near the surface is associated with an arrival of a Canadian cold frontal cloud (Fig. 1). The frontal cloud appears above the shallow low-level cloud. Freezing drizzle ended by this time. Ice/snow particles falling from the seeder cloud likely depleted the supercooled cloud and drizzle drops (Politovich and Bernstein 1995). Formation of a mid- or upper-level cloud layer, for example, with the arrival of a Canadian cold front in the Front Range regions is often a precursor for a cessation of freezing drizzle. General cooling of the cloud top and the presence of a higher level cloud layer eventually suppressed the formation of supercooled drizzle drops on this day.

A precipitation event on 30-31 October 2003 also started as freezing drizzle from a shallow orographic cloud that formed behind a Canadian cold front. Freezing drizzle was reported at the surface for more than 24 hours. The CTTs varied between –10 and –5^{o}C during freezing drizzle. The onset of light snow coincided with a cooling of the cloud top starting at about 1300 UTC on 31 October 2003. The cloud top eventually cooled to nearly –15^{o}C by 1600 UTC. The cloud layer was shallow throughout the event (a depth of 1.6 km). As in the 4 March 2003 case, weak generating cells appeared with the onset of snow yielding an increase in σ_Z. However, the weakening cloud system produced light snow that is barely detectable with the radar. Consequently, $\overline{Z}$ between the periods of freezing drizzle and light snow were similar (Fig. 2). In this case, a horizontal homogeneity in the reflectivity field and a relatively warm cloud top were factors characterizing freezing drizzle.

Freezing drizzle formed behind a quasi-stationary Canadian cold front on 4 January 2005. Freezing drizzle was reported early in the event at the surface observation site in Denver (KDEN) starting at 1533 UTC. Freezing drizzle was soon mixed with "very light snow" according to the KDEN surface precipitation reports. This condition continued until 2100 UTC and produced hazardous road conditions across the Front Range regions. During this time segment, the radar images consisted of a shallow orographic cloud and

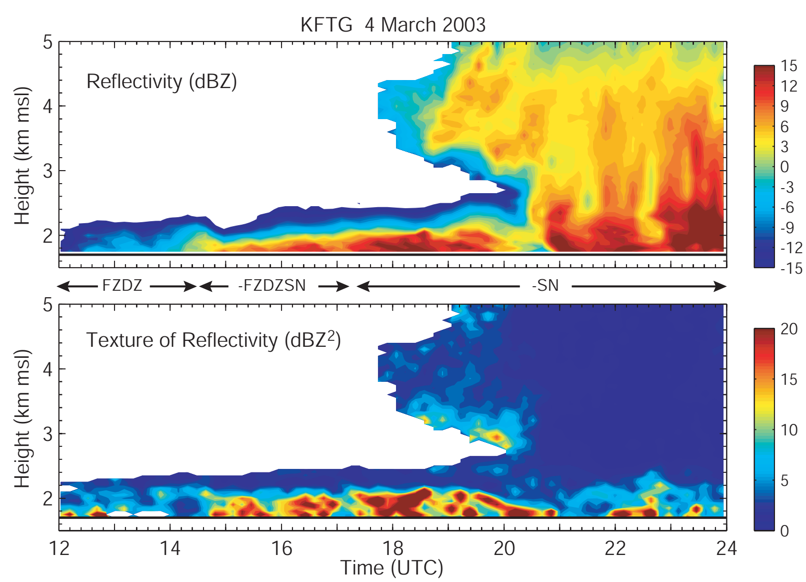

Figure 1: Vertical profiles of radar reflectivity (top) and the texture of reflectivity (bottom) measured with the KFTG radar on 4 March 2003. Precipitation types are also indicated [freezing drizzle (FZDZ), freezing drizzle and light snow (-FZDZSN), and light snow (-SN)].

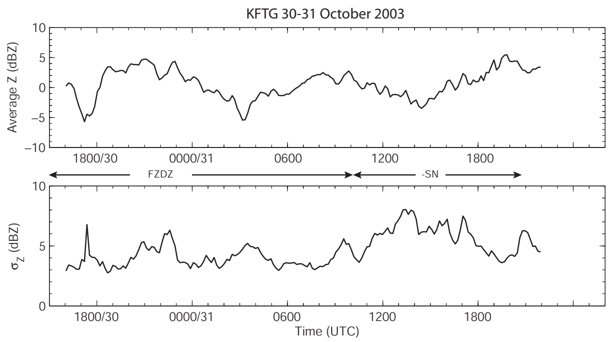

Figure 2: Time histories of average (top) and standard deviation (bottom) of reflectivity measured with the KFTG radar during the 30-31 October 2003 precipitation event.

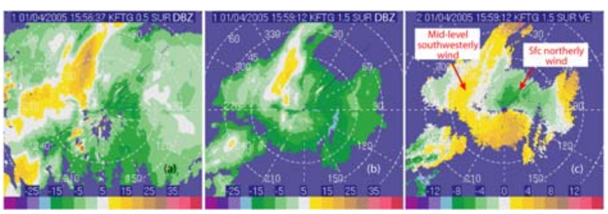

Figure 3: The 360^o-survaillence scans from the KFTG radar showing (a-b) radar reflectivity from 0.5^o and 1.5^o antenna elevations, respectively, and (c) Doppler radial velocity from 1.5^o elevation angle for times shown on 4 January 2005. Range rings are placed every 15 km.

scattered mid-level clouds moving with the southwesterly flow (Fig. 3). Depletion of supercooled drizzle probably took place in limited areas as ice crystals, generated in the mid-level clouds, fell through the low-level cloud layer. The presence of this mid-level cloud and partial depletion of drizzle in the feeder cloud (low-level cloud) produced less uniform reflectivity field with a relatively higher reflectivity (8 dBZ) than the previous freezing drizzle episodes. Freezing drizzle ended, and light snow continued after 2200 UTC. Stratiform precipitation developed by this time returning to the reflectivity field with low texture values and small σ_Z. Although the average texture and σ_Z were similar to those of the previous precipitation stage, CTTs were much less (<$-$30^{o}C), the reflectivity rapidly increased toward ground, and the reflectivity was higher near the surface (>10 dBZ)—all of which are typically not observed in freezing drizzle.

The cloud system on 16 February 2005 over regions surrounding Pueblo, Colorado also consisted of a snow generating mid-level cloud that passed over a preexisting supercooled drizzle cloud. $\overline{Z}$ and σ_Z did not significantly change during the precipitation event even though freezing drizzle possibly became mixed with snow as the mid-level cloud passed over the area. A twin-engine airplane approaching the Pueblo Memorial Airport located approximately 33 km southwest of the radar was involved in a fatal crash. In-flight icing that formed as it descended into the supercooled drizzle cloud is currently being considered as one of the causes of the accident. The 4 January and 16 February 2005 events show difficulty in identifying freezing drizzle based on radar reflectivity and CTT in the presence of mixed-phase precipitation and/or multiple-cloud layer.

The example cases discussed above showed that weak reflectivity with a small texture and σ_Z in the presence of a relatively warm cloud top can suggest the presence of freezing drizzle at the surface (when surface temperature is below freezing). However, the differential $\overline{Z}$, σ_Z, and average value of the texture field in freezing drizzle and snow are not necessarily consistent from one event to another. For example, the uniformity in the reflectivity field during a snow event is similar to that in freezing drizzle when snow is from a stratiform cloud with very little cellularity. The detection of freezing drizzle is further complicated in the presence of multiple cloud layers and in mixed-phase precipitation at the surface. In such cases, the presence of an upper-level cloud layer does not always guarantee the absence of drizzle at the surface, the reflectivity can be as high as 10 dBZ, and cloud tops, as observed from the satellite, are typically much cooler than $-$15^{o}C.

b. Ensemble data

Radar measurements from 17 freezing drizzle and light snow cases obtained from the selected radar systems (Section 2) are examined here. CTTs from satellite (available every 15 or 30 minutes) were interpolated in time to find temperature associated with each radar scan.

The average reflectivity and σ_Z from all precipitation events that were analyzed are plotted against CTT in Fig. 4. The average texture of Z is not shown here because the variations of the texture field with CTT are similar to σ_Z. The overlap between the measurements in freezing drizzle and light snow are significant. However, these statistical values can be explained partly with the cloud vertical structure and CTT. For example, the freezing drizzle episodes from cloud tops cooler than $-$20^{o}C occurred in the presence of multiple-cloud layers; thus, the CTTs are not associated with the temperatures at the top of the low-level cloud. [The presence of multiple cloud layers can be readily verified by examining higher level scans.] When there was a significant directional shear in the horizontal wind field between the two cloud layers, as inferred from the Doppler radial velocity field, the reflectivity was small and horizontally uniform ($\overline{Z}$=~0dBZ, σ_Z<5dB). Perhaps, the seeder-feeder mechanism was not effective in glaciating the low-level cloud layer. On the other hand, the reflectivity field was less uniform (σ_Z>5dB) and $\overline{Z}$ was higher when radar echo top heights were not uniform across the radar site. As in the 4 January 2005 case at KFTG, these cases were commonly associated with freezing drizzle in low-level cloud layer that was only partially affected by the snow generating cells originating at higher altitudes.

Most of the data points associated with CTTs >$-$20^{o}C in Fig. 4 were measured when only a low-level cloud layer was present. These data points with single-layered low-level clouds are plotted in Fig. 5. For a relatively warm precipitation event (CTT>–10^{o}C), freezing drizzle is typically associated with σ_Z of nearly 4 dBZ (Fig. 6). Although only 18 data points are from light snow cases compared with 110 points for freezing drizzle, this is about 3 dBZ lower than in light snow for similar magnitudes of reflectivity. For cold precipitation events (CTT<–10^{o}C), reflectivity remains near 0 dBZ in freezing drizzle; whereas the reflectivity measurements in snow shifts to higher values (Fig. 5). The larger reflectivity is partly due to the fact that ice generation occurs rapidly near the cloud top, and particles grow to appreciable sizes as they descend through the cloud. Consequently, the vertical gradient of reflectivity is larger than that in freezing drizzle. The horizontal uniformity in the two precipitation types are similar. Uniform reflectivity fields in light snow cases come from the presence of stably stratified clouds, typically, in the absence of ice generating cells and snow bands. Light snow between 1700 and 1800 UTC on 4 March 2003 is an example of this case. The data shows that the occurrence of freezing drizzle decreases as the cloud top cools for single-layered cloud cases (Fig. 5) consistent with the findings from Geresdi et al. (2005).

Consistent with findings from the case studies in the previous section, the ensemble data indicate that a freezing drizzle detection scheme should associate a weak and a relatively smooth reflectivity field and warm cloud top (>-10^{o}C) with freezing drizzle. The echo patterns often overlap with light snow, but the likelihood of light snow increases when σ_Z is >5dBZ for clouds in the warm regime and when $\overline{Z}$ is >5dBZ in the cold regime. These general rules do not apply in the presence of multiple cloud layers.

4. Measurements of drizzle with a polarimetric radar

Lead by the National Weather Service, a program to add polarimetric capability to the network of WSR-88Ds is currently underway (Ryzhkov et al. 2005). Because polarimetric measurements are sensitive to particle size, shape, orientation, phase, and density, the measurements would provide more insight regarding particle types than currently available with radar reflectivity alone.

One of the added measurements to the polarimetric WSR-88D is differential reflectivity (Z_{DR}). Z_{DR} is sensitive to particle bulk density, shape, and canting angle and can be interpreted as the reflectivity-weighted mean axis ratio of the illuminated hydrometeors. Z_{DR} is zero for particles that are spherical or have a random distribution of orientations. Z_{DR} typically ranges from 0.2 to 3 dB for rain and increases with drop size and rain intensity. Pristine ice crystals fall with their major axes near horizontal and can have Z_{DR} values as large as 2 to 5 dB depending on crystal type. Z_{DR} for low density aggregates are small (0 to 0.5 dB). Although the capability of Z_{DR} to discriminate between rain and snow has been previously explored (e.g., Ryzhkov and Zrnic 1998) there has been few detailed studies contrasting return signals from drizzle and snow

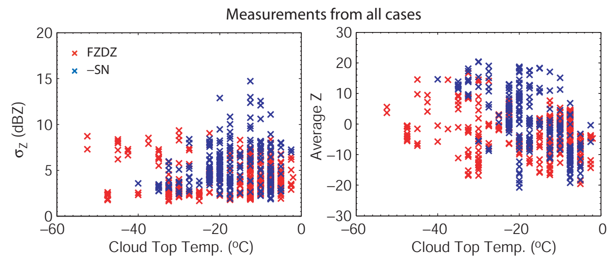

Figure 4: Standard deviation and average reflectivity versus cloud top temperatures from all freezing drizzle (FZDZ) and light snow (-SN) cases considered in this study. Red (blue) crosses are for measurements during freezing drizzle (light snow).

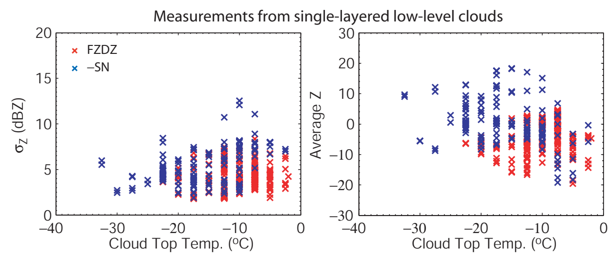

Figure 5: Same as Fig. 4 except for single-layered clouds.

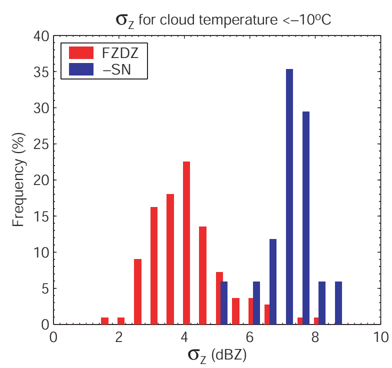

Figure 6: Frequency distributions of standard deviation of reflectivity in warm regime (CTT>-10^{o}C).

(e.g., Reinking et al. 1997; Reinking et al. 2002). Here, we present measurements of differential reflectivity (Z_{DR}) and reflectivity from horizontal polarization (Z_H) collected from drizzle and light snow with NCAR's S-band polarimetric radar (S-Pol) during the second phase of the Improvement of Microphysical Parameterization through Observational Verification Experiment (Stoelinga et al. 2003).

Figures 7 and 8 show scatter plots of Z_H and Z_{DR} measurement pairs and the distributions of Z_{DR} just below and above the melting layer. The measurements were obtained in light orographic precipitation. The Z_H and Z_{DR} are small below the melting layer suggesting that the drops were small (Fig. 7a). The absence of a bright band in the reflectivity cross sections also

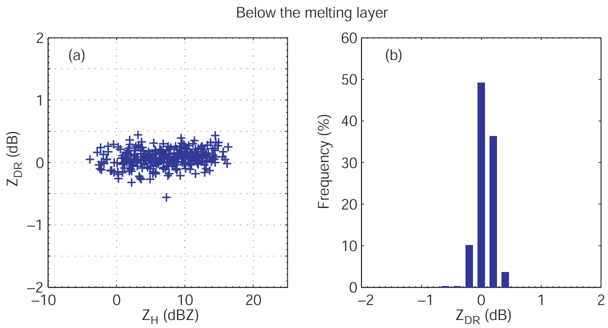

Figure 7: (a) Scatter plot of Z_{DR} and Z_H from a selected area below the melting layer, and (b) a frequency distribution of Z_{DR}. The measurements were collected between 1202 and 1204 UTC on 28 November 2001 during IMPROVE II.

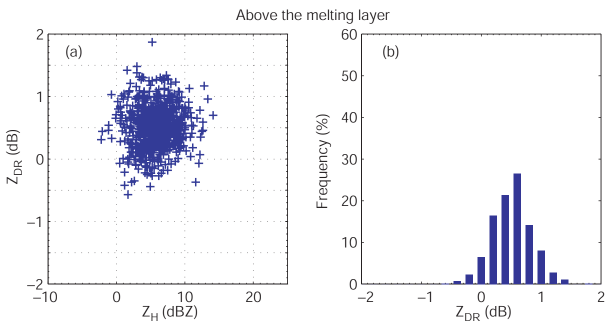

Figure 8: Same as Fig. 7 but for measurements above the melting layer.

indicated that drops below the melting layer were probably drizzle. The Z_{DR} distribution for drizzle is strongly peaked near 0 dB (Fig. 7b) because they are essentially spherical. Although this is not a case of freezing drizzle, the radar returns are similar. Compared to drizzle, Z_{DR} is higher in the ice layer (~0.6 dB) for similar magnitude of Z_H, indicating that the particles are less spherical in the mean (Fig. 8). A broad distribution of Z_{DR} in the ice layer was also common among datasets examined in this study. These differential Z_{DR} signatures in drizzle and snow give prospects of enhanced freezing drizzle detection with a polarimetric WSR-88D.

5. Summary and concluding remarks

The WSR-88D radar measurements obtained in freezing drizzle were discussed. The radar returns from freezing drizzle were typically weak (< 5dBZ) and horizontally uniform (σ_Z < 4 dBZ). The ensemble data from a number of freezing drizzle and light snow cases showed that the echo patterns from the two types of precipitation overlap. However, the data also indicated that differential average reflectivity and its horizontal structure are, to some degree, related to cloud top temperature (CTT) when only a low-level cloud was present. For similar magnitudes, the reflectivity is typically more horizontally uniform in freezing drizzle than in light snow during warm events (CTT>–10^{o}C). The average reflectivity near the surface and the rate of reflectivity increase toward ground are larger in cold events (CTT<–10^{o}C) for light snow as ice generation becomes active and ice crystals rapidly grow; whereas the radar returns in freezing drizzle continue to have a relatively small standard deviation and weak reflectivity. Freezing drizzle formation is limited for much cooler cloud temperatures (CTT<–20^{o}C). Radar echo patterns for freezing drizzle largely overlapped with light snow when multiple cloud layers were present. In these cases, CTT and reflectivity were not sufficient to discriminate between freezing drizzle and snow.

Comparisons of Z_H and Z_{DR} pairs in drizzle and ice layers revealed that Z_{DR} in the ice layer differ in two ways: (1) it is larger for a specified Z_H; and (2) the range of values at a specific Z_H is larger. These differential signatures in drizzle and snow should enhance the freezing drizzle detection when polarimetric WSR-88Ds become available. Polarimetric measurements (not only Z_{DR}) add more insight regarding the particle types and are particularly useful for precipitation events in the cold regime or with multiple cloud layers in which cases the particle discrimination criteria based on CTT and reflectivity do not apply.

Acknowledgement: This research is in response and funding by the Federal Aviation Administration (FAA). The views expressed are those of the authors and do not necessarily represent the official policy or position of the U.S. government.

References

Bernstein, B. C., 2000: Regional and local influences on freezing drizzle, freezing rain, and ice pellet events. *Wea. Forecasting*, **15**, 485-508.

Geresdi. I., R. Rasmussen, W. Grabowski, and B. Bernstein, 2005: Sensitivity of freezing drizzle formation in stably stratified clouds to ice processes. *Meteorol. Atmos. Phys.*, **88**, 91-105.

Kessinger, C., S. Ellis, and J. Van Andel, 2003: The radar echo classifier: A fuzzy logic algorithm for the WSR-88D. Preprints, *3rd Conference on Artificial Applications to the Environmental Science*, Long Beach, CA, Amer. Meteor. Soc.

Politovich, M. K., and B. C. Bernstein, 1995: Production and depletion of supercooled liquid water in a Colorado winter storm. *J. Appl. Meteor.*, **34**, 2631-2648.

Reinking, R. F., S. Y. Matrosov, B. E. Martner, and R. A. Kropfli, 1997: Dual-polarization radar to identify drizzle, with applications to aircraft icing avoidance. *J. Aircraft*, **34**, 778-784.

_____, _____, R. A. Kropfli, and B. W. Bartram, 2002: Evaluation of a 45^o slant quasi-linear radar polarization state for distinguishing drizzle droplets, pristine ice crystals, and less regular ice particles. *J. Atmos. Oceanic Technol.*, **19**, 296-321.

Ryzhkov, A. V., and D. S. Zrnic, 1998: Discrimination between rain and snow with a polarimetric radar. *J. Appl. Meteor.*, **37**, 1228-1240.

_____, T. J. Schuur, D. W. Burgess, P. L. Heinselman, S. E. Giangrande, and D. S. Zrnic, 2005: The Joint Polarization Experiment: Polarimetric rainfall measurements and hydrometeor classification. *Bull. Amer. Meteor. Soc.*, **86**, 809-824.

Stoelinga, M. T., and co-authors, 2003: Improvement of microphysical parameterization through observational verification experiment. *Bull. Amer. Meteor. Soc.*, **84**, 1807-1826.